Received: 8 October 2018 | Revised: 11 March 2019 | Accepted: 15 March 2019

DOI: 10.1002/hbm.24586

RESEARCH ARTICLE

WILEY

The cingulum and cingulate U-fibers in children and adolescents with autism spectrum disorders

Janice Hau | Saba Aljawad | Nicole Baggett | Inna Fishman | Ruth A. Carper | Ralph-Axel Müller

Brain Development Imaging Laboratories, Department of Psychology, San Diego State University, San Diego, California

Correspondence
Ruth A. Carper, Brain Development Imaging Laboratories, Department of Psychology, San Diego State University, San Diego, CA.
Email: rcarper@sdsu.edu

Abstract

The cingulum is the major fiber system connecting the cingulate and surrounding medial cortex and medial temporal lobe internally and with other brain areas. It is important for social and emotional functions related to core symptomatology in autism spectrum disorders (ASDs). While the cingulum has been examined in autism, the extensive system of cingulate U-fibers has not been studied. Using probabilistic tractography, we investigated white matter fibers of the cingulate cortex by distinguishing its deep intra-cingulate bundle (cingulum proper) and short rostral anterior, caudal anterior, posterior, and isthmus cingulate U-fibers in 61 ASD and 54 typically developing children and adolescents. Increased mean and radial diffusivity of the left cingulum proper was observed in the ASD group, replicating previous findings on the cingulum. For cingulate U-fibers, an atypical age-related decline in right posterior cingulate U-fiber volume was found in the ASD group, which appeared to be driven by an abnormally large volume in younger children. History of repetitive and restrictive behavior was negatively associated with right caudal anterior cingulate U-fiber volume, linking cingulate motor areas with neighboring gyri. Aberrant development in U-fiber volume of the right posterior cingulate gyrus may underlie functional abnormalities found in this region, such as in the default mode network.

KEYWORDS
autism, cingulum, diffusion imaging, tractography, U-fibers, white matter

1 | INTRODUCTION

Autism spectrum disorders (ASDs) are a group of neurodevelopmental disorders characterized by persistent deficits in social communication and interaction, and unusual patterns of restricted interests and repetitive behaviors (American Psychiatric Association, 2013). ASDs are understood to involve abnormal brain connectivity and alterations in the normal integration of brain activity (Belmonte et al., 2004). There has been considerable focus on functional connectivity, but a number of studies have applied diffusion tensor imaging (DTI) to examine structural connectivity in ASDs identifying micro- and macrostructural abnormalities in the white matter, with some consistent results (albeit almost exclusively within long fiber tracts) (Ameis & Catani, 2015; Aoki, Abe, Nippashi, & Yamasue, 2013; Travers et al., 2012).

One of the white matter pathways that has consistently been implicated in autism is the cingulum. The cingulum subserves the cingulate and surrounding medial cortex and the medial temporal lobes, areas important for social cognition (Amodio & Frith, 2006), emotion processing (Bush, Luu, & Posner, 2000), and motor control (Paus, 2001). Reduced fractional anisotropy (FA) and/or higher diffusivity measures in the cingulum—indicating compromised microstructure—have been reported in children, adolescents and adults with ASDs (Ameis et al., 2013; Catani et al., 2016; Ellmore, Li, Xue, Wong, & Frye, 2013; Fitzgerald, Gallagher, & McGrath, 2016; Ikuta et al., 2014;

 © 2019 Wiley Periodicals, Inc.

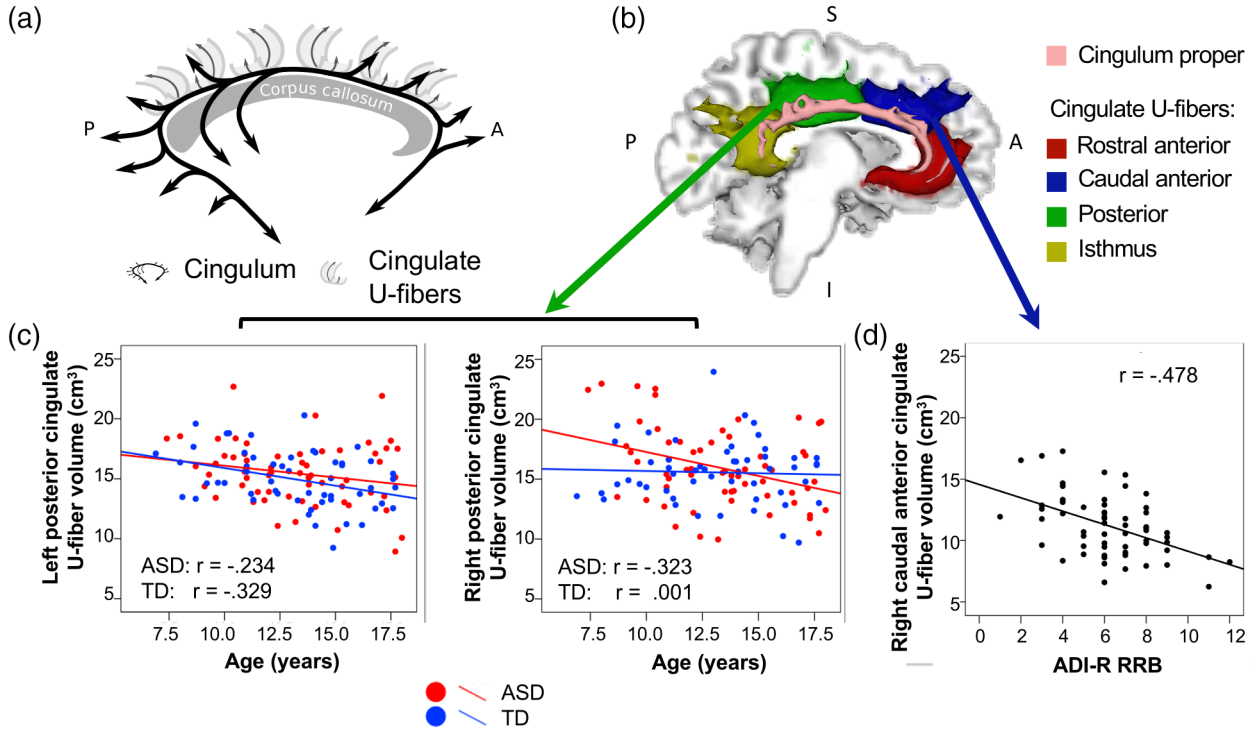

FIGURE 1 a–d. (a) Schematic representation of the cingulum (in black), defined as fibers that enter the main fiber bundle and travel longitudinally along it before exiting, and cingulate U-fibers (in gray), defined as short fibers that connect the cingulate cortex with neighboring cortex—these may cross the main bundle portion of the cingulum but do not travel long distances within it. (b) Examples of cingulum proper (pink) and rostral anterior (red), caudal anterior (blue), posterior (green), and isthmus (yellow) cingulate U-fiber tracts of the left hemisphere (medial view) are shown for an ASD participant (age 17 years). (c) Left posterior cingulate U-fiber volume decreased with age in ASD and TD (left panel). Right posterior cingulate U-fiber volume decreased with age in the ASD group only (right panel). (d) Tract volume of the right caudal anterior cingulate U-fiber was negatively associated with the ADI-R repetitive subscore in the ASD group.
Abbreviations: ADI-R, autism diagnostic interview-revised ; ASD, autism spectrum disorder

Koolschijn, Caan, Teeuw, Olabarriaga, & Geurts, 2016), contrasting with higher FA in toddlers with ASDs (Billeci, Calderoni, Tosetti, Catani, & Muratori, 2012; Weinstein et al., 2011; Xiao et al., 2014), though potential confounds of head motion (Koldewyn et al., 2014; Yendiki, Koldewyn, Kakunoori, Kanwisher, & Fischl, 2013) may not have been fully considered in some of these. Ikuta et al. (2014) additionally showed a group by age interaction in adolescents and young adults (13–23 years) where the typical age-related increase in cingulum FA was not present in the ASD group. While the direction of microstructural differences found in the cingulum in ASD studies is generally consistent for a given age group, the laterality of effects is less clear. Variability in the anatomical definitions of the cingulum (discussed below), methods for obtaining cingulum tract measures, participants' age range, and sample size, as well as heterogeneity of the clinical phenotype, are likely to contribute to inconsistencies.

In healthy controls, higher cingulum FA has been linked to improved executive functions (Bettcher et al., 2016; Metzler-Baddeley et al., 2012), and its subgenual division has been associated with regulating attention to negative emotional stimuli (Keedwell et al., 2016). Only a handful of studies have examined the relationship between structural measures of the cingulum and clinical indices in ASDs. One small sample study reported that decreased cingulum FA was associated with greater impairment in behavioral regulation (measured with the behavior rating inventory of executive function) in young adults with ASDs (Ikuta et al., 2014). Despite the cingulum's hypothesized role in social cognition, findings have been inconsistent in ASDs. A recent ASD study found no relationship between autism socio-communicative symptoms and cingulum micro- or macrostructural measures (Catani et al., 2016), although a negative relationship between FA and social awareness (measured with the Social Responsiveness Scale) has been reported in young adults with ASDs (Chiang, Chen, Lin, Tseng, & Gau, 2017).

Like many white matter pathways, the cingulum's detailed anatomy is complex and often oversimplified. Burdach described the pathway as a pair of bundles running from the basal surface of the frontal lobe through the parietal lobe and bending back anteriorly to the temporal pole, forming a “ring-like belt” (resembling the *cingulum militare*) throughout the medial brain (Schmahmann & Pandya, 2006). However, it is likely that the cingulum consists of multiple sub-bundles, with different endpoints and different functions. Fibers enter and exit the pathway along the length of the bundle as can be seen in Figure 1a making them difficult to follow and fully describe in post-mortem dissection. Tracer studies in the primate brain have confirmed the existence of both fibers that do not connect with the cingulate cortex and fibers with afferent and/or efferent connections in the cingulate cortex, that travel through the main cingulum bundle in the

deep white matter (see Heilbronner & Haber, 2014). In contrast, cingulate U-fibers, located in superficial white matter (nearer to the cortex), connect the cingulate cortex with its adjacent areas. Cingulate U-fibers are in proximity to the cingulum bundle and may cross it, but unlike cingulum fibers, do not travel along it (Figure 1a). As a reflection of this anatomical complexity, the term "cingulum" has often been interpreted as the entire system of axons connecting the cingulate gyrus, collectively resembling an "Indian war bonnet" (Yakovlev and Locke, 1961). In diffusion-weighted imaging (DWI), most studies focus on the long portion of the cingulum constituting the main bundle, here referred to as the *cingulum proper*.

Cingulate U-fibers have largely been overlooked in neuroanatomical and neuroimaging studies of autism. These short U-shaped fibers support efficient neural transmission between the cingulate cortex and medial parts of the orbitofrontal, prefrontal, parietal and temporal cortices, and may have particular importance in moderating limbic influences on cognitive, motor, and social functioning affected in ASDs. Evidence of abnormality in the superficial white matter (SWM; corresponding to superficially located U-fibers) as opposed to deep white matter (DWM; corresponding to deep fiber pathways that travel longer distances in the brain) in ASDs has been reported. In a series of postmortem studies, Zikopoulos and colleagues divided white matter underlying the anterior cingulate cortex in ASDs into superficial and deep compartments and sorted axons by their inner diameter. They found a pronounced increase in the number of small-caliber axons in SWM and fewer large-caliber axons in DWM in ASDs compared with controls (Zikopoulos & Barbas, 2010; Zikopoulos, Garcia-Cabezas, & Barbas, 2018). A few neuroimaging studies have also reported abnormality in SWM in autism, including enlarged SWM across all lobes (Herbert et al., 2004) and reduced FA and/or increased mean diffusivity in frontal, temporal and parietal SWM areas (Shukla, Keehn, Smylie, & Müller, 2011; Sundaram et al., 2008; Thompson et al., 2017) in young children up to middle-age adults with ASDs. Thompson et al. (2017) segmented U-fibers of the hand region and further showed that its microstructural alterations were associated with fine motor impairment in ASD adults. Another study used a novel approach using a population-derived U-fiber atlas and found reduced connectivity in ASD in select frontal, temporal, parietal U-fibers that were associated with symptom severity (d'Albis et al., 2018). Studying the U-fibers in addition to the cingulum proper may provide further insight into how this white matter area supporting the limbic system may be related to core ASD symptoms.

Based on extensive evidence, implicating structure and function of the cingulate region in ASDs described above, the present study investigated the micro- and macrostructural properties of the left and right cingulum proper and U-fibers of the rostral anterior, caudal anterior, posterior, and isthmus cingulate cortex, including their developmental trajectories, in children and adolescents with ASDs and a typically developing comparison group. The aims were to: (a) replicate findings of altered microstructure in the cingulum proper in ASDs in a relatively large low-motion sample, (b) investigate cingulate U-fibers to test the hypothesis of increased U-fiber volume, reflecting an increased number of SWM axons underlying the cingulate cortex in ASDs as shown in postmortem studies, and (c) examine how cingulum proper and cingulate U-fiber micro- and macrostructural measures relate to clinical indices and autism symptoms.

2 | METHODS

2.1 | Participants

A total of 102 children and adolescents with ASDs and 77 typically developing (TD) participants, aged 7–18 years, were enrolled for this study. Seventeen ASD and eight TD participants were excluded for technical failures or incomplete diffusion sequence. After excluding participants for excessive motion artifacts and/or poor diffusion image quality (12 ASD, 8 TD), incomplete or poor T1-weighted data (two ASD, two TD), incidental MRI findings (three ASD, two TD) or not meeting TD inclusionary criteria (one with adopted ASD siblings, two suspected of having other clinical disorders), and excluding seven ASD participants to match the diagnostic groups on motion (as described below), the final sample consisted of 61 ASD and 54 TD participants.

ASD diagnoses were based on DSM-5 (American Psychiatric Association, 2013) criteria with supporting assessments of the autism diagnostic observation schedule, second edition (ADOS-2) (Lord, Rutter, DiLavore, & Risi, 2002) and autism diagnostic interview-revised (ADI-R; Le Couteur, Lord, & Rutter, 2003), and were confirmed by a clinical psychologist (Inna Fishman) experienced in the diagnosis of ASDs. Participants with a history of genetic or neurological conditions (e.g., epilepsy, Fragile-X, and tuberous sclerosis) were excluded during screening. ASD participants with comorbid attention deficit hyperactivity disorder (ADHD), obsessive–compulsive disorder (OCD), or anxiety disorders were not excluded because of the high prevalence of these conditions in children and adolescents with ASDs (Simonoff et al., 2008). Further exclusion criteria for TD participants were personal or family history of autism and personal history of any other neurological, developmental, or psychiatric conditions. Overall, cognitive functioning was assessed by the Wechsler abbreviated scale of intelligence, second edition (WASI-II) (Wechsler, 1999). In addition to the ADOS-derived indices of social behavior available only for ASD participants, social functioning was assessed in all participants using the parent report-based social responsiveness scale (SRS; Constantino, 2002). Executive function was additionally assessed using the behavior rating inventory of executive function (BRIEF-2; Gioia, Isquith, Guy, & Kenworthy, 2016). Hand preference was assessed with the Edinburgh Handedness Inventory (Oldfield, 1971). Informed assent and consent were obtained from all participants and their caregivers, respectively, in accordance with the University of California, San Diego, and San Diego State University Institutional Review Boards.

2.2 | MRI data acquisition

Imaging data were acquired on a GE Discovery MR750 3.0 T scanner with an eight-channel head coil. Diffusion-weighted images were collected using an echo planar pulse sequence with full head coverage,

encoded for 61 noncollinear diffusion directions at b = 1,000 s/mm^2, and one at b = 0 s/mm^2 (TR = 8,500 ms; TE = 84.9 ms; flip angle = 90°; FOV = 240 mm; 1.88 × 1.88 × 2 mm^3 resolution) with a matching field map to correct for magnetic field inhomogeneities (2D GRASS; TR = 1,097 ms; TE = 9.5 ms; flip angle = 45°). Additionally, depending on the date of scan, for improved field inhomogeneity correction two pairs of images with no diffusion weighting were collected with anterior–posterior and posterior–anterior phase-encoding directions (collected for 49% of ASD and 48% of TD participants). A high-resolution anatomical image was also obtained for each participant using a T1-weighted fast spoiled gradient echo sequence (TR = 8.108 ms; TE = 3.172 ms; flip angle = 8°; 172 slices; 1 mm^3 resolution).

2.3 | Anatomical parcellation

Cortical regions were automatically parcellated in each individual's T1-weighted image using FreeSurfer (http://surfer.nmr.mgh.harvard.edu/) and labeled with the Desikan–Killiany template (Desikan et al., 2006). Anatomical parcellations were inspected for quality control and manually edited when necessary. Each individual's set of parcellated regions was registered to their distortion-corrected native diffusion space using a boundary-based linear registration (Greve & Fischl, 2009). Selected regions were used as seed, target and exclusion masks for tractography as described below.

2.4 | DWI preprocessing

Preprocessing was performed using the FMRIB Software Library 5.0.9 (FSL, http://www.fmrib.ox.ac.uk/fsl/). Diffusion-weighted images underwent correction for susceptibility-induced off-resonance distortions using either a field map (fugue) or, if available, opposite phase-encoded non-diffusion weighted scan pairs (top-up; Andersson, Skare, & Ashburner, 2003). Estimating the off-resonance field from distortion in opposing directions (opposite phase-encoded scan pairs) improves the sampling density even in distorted areas, such as the temporal poles. Eddy current distortions and head motion were corrected using the FSL eddy tool (Andersson & Sotiropoulos, 2016). To minimize the effect of motion-induced signal dropout common in diffusion acquisitions, an integrated outlier replacement step within eddy identified slices four or more standard deviations below their expected average intensity and replaced them with a model-based estimate (Andersson, Graham, Zsoldos, & Sotiropoulos, 2016). The b-matrix of each participant was rotated to account for motion correction and was used in subsequent processing. As our diffusion data were preprocessed with one of two distortion correction methods (fugue or top-up), an additional "pipeline" variable was included in all data analyses to account for potential differences due to preprocessing pipeline.

2.5 | DWI tractography

Probability distribution functions of local fiber directions at each voxel were built using a ball-and-stick model to resolve fiber crossings of up to three directions (bedpostX; Behrens, Berg, Jbabdi, Rushworth, & Woolrich, 2007). Probabilistic tractography (probtrackx2; Behrens et al., 2003; Behrens et al., 2007) was performed by sampling from the distribution of directions in the subjects' diffusion space using the default parameters starting from seed regions. For the cingulum proper (Figure 1b), the seed region was the subject-specific cingulate cortex (combination of all four FreeSurfer-derived cingulate cortex subdivisions) of each hemisphere, and an exclusion zone consisting of the brain outside the ipsilateral cingulate cortex, parahippocampal and entorhinal gyri was used to restrict streamlines to core areas of the cingulum bundle. In addition, a small rectangular ROI was delineated on two consecutive coronal slices in standard Montreal Neurological Institute space (center of gravity located at: x = 1, y = −2.5, z = 11.5 mm), and was warped to each subject's diffusion space, to exclude cingulate streamlines entering the fornix, given its proximity. It was determined that two coronal slices were necessary in order to have sufficient coverage of the area after transformation from MNI to subject space. Tract thresholds were chosen after evaluating a range of possible values and visually comparing results with known neuroanatomy. A conservative threshold of 20% of the maximum value was used to ensure that only the core of the cingulum proper bundle was selected (i.e., excluding U-fibers). For the cingulate U-fibers (Figure 1b), seeding was done from each of: rostral anterior, caudal anterior, posterior, and isthmus cingulate regions. Tracks running longitudinally along the cingulate gyrus (cingulum proper) were excluded by using the adjacent cingulate cortical regions and parahippocampal gyrus, dilated one voxel into the white matter, as exclusion areas. These were dilated one voxel into the underlying white matter, which was sufficient to prevent streamlines from propagating along the cingulate cortex. U-fiber tracts were thresholded at 1% of the maximum number of streamlines traversing a voxel, after evaluation of a range of possible values. For both tracts, streamlines entering the thalamus or contralateral hemisphere were also excluded.

Diffusion measures including FA, mean, radial, and axial diffusivity (MD, RD, and AD) were computed with a standard linear regression fit (dtifit) and tract measures were obtained by averaging across voxels occupied by the tract. Tract volume was measured in mm^3 in the native diffusion space.

2.6 | Head motion and group matching

Motion in DWI scans presents a well-known methodological challenge particularly in studies of clinical populations such as ASDs. Matching groups on quantitative measures of head motion has been shown to reduce spurious effects and increase effect sizes in group analyses (Solders, Carper, & Müller, 2017; Yendiki et al., 2013). Root mean square displacement (RMSD) of diffusion-weighted volumes (relative to the non-diffusion weighted volume) and the percentage of slices affected by signal dropout (number of slices affected by signal dropout/total number of slices) were used to quantify and match the groups on head motion. RMSD was calculated without translation in the phase-encoding direction to remove movement confounded with eddy currents during the DWI scans and averaged to produce an

estimate of bulkhead motion (Andersson & Sotiropoulos, 2016). Scans with ≥3% slice signal dropout were excluded.

Differences between diagnostic groups for age, SRS, intelligence quotient, RMSD, and percentage of slice dropout were assessed using *t*-tests, and sex, and handedness were compared using chi-square tests. After motion matching, diagnostic groups did not significantly differ on age, sex, handedness, non-verbal IQ, RMSD, or percentage of slice dropout (Table 1). As expected, BRIEF-2 and SRS scores were significantly higher in ASD compared with the TD group (both $p < .001$), while verbal IQ was significantly lower in the ASD group ($p = .01$).

2.7 | Statistical analysis

Statistical analyses were performed using the Statistical Program for the Social Sciences version 24 (SPSS, Chicago, IL). Linear regression analysis was used to test for group and age main effects, and group by age interactions on diffusion (FA, MD, RD, and AD) and volume measures of the cingulum proper. Given the large number of comparisons for cingulate U-fiber tracts, repeated measures ANCOVAs for the left and right hemisphere were performed to test for group and age main effects, and group by age interactions on diffusion and volume measures of the U-fiber tracts. Percentage slice dropout and a pipeline variable (coding for distortion-correction method) were included as nuisance variables in all analyses. False discovery rate (FDR) correction was applied separately to the cingulum proper (left and right tracts in one family) and U-fiber tracts (all segments included in one family) to correct for multiple comparison tests using a q-value of .05. Follow-up partial correlation analyses were run to investigate significant hemisphere × age and hemisphere × group × age interactions on groups and/or hemispheres separately, controlling for percentage slice dropout and pipeline. To examine, behavioral correlates of the cingulum proper and cingulate U tracts, partial correlations were run between behavioral measures (ADOS-2 subscales: Social Affect [SA] and Restricted and Repetitive Behaviors [RRB]; ADI-R subscales: Social, Communication, and RRB; BRIEF-2 general executive composite [GEC] index; SRS Total scores) and tract measures (restricted to FA, MD, and volume measures to limit number of tests), controlling for age, percentage slice dropout and pipeline. Partial correlations with BRIEF-2 GEC and SRS Total were run separately for each group, and with ADOS-2 and ADI-R scores for ASD group only. FDR correction was applied to adjust the significance level for multiple tests using a q-value of .05 (Benjamini & Hochberg, 1995).

3 | RESULTS

The cingulum proper and cingulate U-fibers were successfully extracted in all subjects. The cingulum proper was situated more centrally (deep) within the cingulate white matter relative to the cingulate U-fiber tracts (Figure 1b) consistent with known anatomy (Maldonado, Mandonnet, & Duffau, 2012; Schmahmann & Pandya, 2006).

The results of linear regression analyses for cingulum proper are summarized in Table 2. There were main effects of age, with the left cingulum proper showing increasing volume ($p = .016$) and decreasing

TABLE 1 Participant characteristics and group matching

	ASD ($n = 61$)		TD ($n = 54$)		
	Mean ± *SD* [range]		Mean ± *SD* [range]		p^a
Gender (M/F)	48/13		45/9		.56
Handedness (R/L)	52/9		47/7		.81
Age (years)	13.3 ± 2.8	[7.4–18.0]	13.1 ± 2.9	[6.9–17.7]	.83
Verbal IQ	98 ± 18	[56–147]	105 ± 12	[73–127]	.01
Non-verbal IQ	104 ± 19	[53–140]	105 ± 14	[62–137]	.64
Full-scale IQ	101 ± 18	[61–141]	106 ± 13	[79–130]	.10
ADOS-2 Social Affect	11.1 ± 4.1	[4–20]	n/a		
ADOS-2 Repetitive Behavior	3.4 ± 2.0	[0–8]	n/a		
ADOS-2 Symptom Severity	7.8 ± 1.9	[3–10]	n/a		
BRIEF-2 GEC	71 ± 10	[43–88]	45 ± 6	[37–56]	<.001
SRS Total	83 ± 10	[62–100]	43 ± 6	[35–58]	<.001
Slice dropout (%)	0.66 ± 0.50	[0.02–2.07]	0.60 ± 0.43	[0.07–1.88]	.48
RMSD (head motion)	1.10 ± 0.68	[0.28–4.31]	1.06 ± 0.62	[0.26–3.85]	.76

Note. Before matching the groups on motion, the percentage of slice dropout was significantly higher in the ASD group (8% difference, $p = .039$), as expected. We tightly matched groups on motion by removing seven ASD subjects with the highest percentage of slice dropout from analyses to achieve a group difference below 3% on both RMSD and percentage of dropout. Nineteen participants with ASDs reported having comorbid psychiatric conditions, including attention-deficit/hyperactivity disorder (10), depression (6), and anxiety (10), with five participants reporting more than one comorbid condition. For six ASD participants, information on potential comorbidities was unavailable.

Abbreviations: ADOS-2, Autism Diagnostic Observation Schedule, second edition; ASD, autism spectrum disorder; BRIEF-2, Brief Rating Inventory of Executive Function; RMSD, root mean square displacement; SRS, Social Responsiveness Scale.

[a]*t*-tests; chi-square test for gender and handedness.

AD (p = .030), and the right cingulum proper showing decreasing MD (p < .001), RD (p = .005), and AD (p = .001). We found significant group effects in left cingulum proper, with increased RD (p = .023) and MD (p = .041) in the ASD group compared to controls. No significant group by age interactions were detected for any of the tract measures.

For the behavioral partial correlations, summarized in Table S1, MD in right cingulum proper was negatively correlated with ADI-R Communication (r = −.303, p = .022) and RRB (r = −.277, p = .037) in the ASD group (Figure S1A) as well as with SRS Total (r = −.273, p = .038; Figure S1C. BRIEF-2 GEC was negatively associated with right cingulum proper MD (r = −.393, p = .011) in ASD but not TD where the trend was reversed (r = .302, p = .07). For left cingulum proper MD associations with BRIEF-2 GEC were positive for both groups but significant only for TD (r = .357, p = .03; Figure S1B). None of these behavioral partial correlations, however, survived FDR correction. No significant relationships were found between cingulum proper tract measures and any of the other behavioral indices in either group. To test for group differences in slopes, follow-up regression analyses were run for SRS Total and GEC with the associated tract measures. There was a significant interaction between group and GEC score on right cingulum proper MD (p = .002).

The results of the four repeated measures ANCOVAs performed on cingulate U-fibers are summarized in Table 3. There were significant main effects of hemisphere for rostral anterior (p = .01, left>right) and caudal anterior (p = .002, right>left) cingulate U-fiber volume. We found hemisphere by age interactions for rostral anterior cingulate U-fiber MD (p = .004) and RD (p = .008). Follow-up partial correlations revealed MD and RD decreased with age in the right hemisphere (MD: r = −.210, p = .026; RD: r = −.201, p = .032) but not in the left (MD: r = 0.003, n.s.; RD: r = .010, n.s.). A main effect of age was significant for posterior cingulate U-fiber volume (p = .006, η^2 = .068) in the negative direction (r = −0.223, p = .001). A significant hemisphere by group by age interaction was detected in posterior cingulate U-fiber volume (p = .011). Follow-up partial correlations revealed a significant decrease of right posterior cingulate U-fiber volume with age in the ASD group (r = −.323, p = .013) but not in TD (r = .001, n.s.), whereas left posterior cingulate U-fiber volume decreased with age in TD (r = −.329, p = .017) and approached significance in ASD (r = −.234, p = .074; Figure 1c).

Behavioral partial correlations for U-fiber measures are summarized in Table S1. After FDR correction, ADI-R RRB subscore was negatively correlated with right caudal anterior cingulate U-fiber volume (r = −.478, p < .001) within the ASD group (Figure 1d). Several behavioral correlations were significant at the sub-threshold level (i.e., did not survive FDR correction). Right rostral anterior (r = −.369, p = .005) and left posterior (r = −.409, p = .002) cingulate U-fiber volumes were negatively correlated with ADI-R RRB subscore in ASD (Figure S2A). Right rostral anterior cingulate U-fiber FA was positively correlated with ADOS-2 RRB (r = .305, p = .037; Figure S2A). ADI-R Social subscore was positively correlated with left posterior cingulate U-fiber volume (r = .32, p = .015) and negatively correlated with FA for that tract (r = −.284, p = .032; Figure S2B). SRS Total was positively correlated with left rostral (r = .373, p = .008) and caudal (r = .321, p = .023) anterior cingulate U-fiber volume in TD but not in ASD participants (Figure S3A). In the TD group BRIEF-2 GEC was negatively associated with left posterior cingulate U-fiber FA (r = −.385, p = .019) and positively associated with MD for the same tract (r = .332, p = .045), and was positively associated with left caudal anterior cingulate U-fiber MD (r = .365, p = .026; Figure S3B). Follow-up regression analyses testing for group differences in slopes on SRS Total and GEC did not reveal significant interactions.

TABLE 2 Linear regression analysis results of cingulum proper

	Age		Group		Group × age
Tract/measure	**β**	***p***	**β**	***p***	***p***
Left cingulum proper					
FA		n.s.		n.s.	n.s.
MD		n.s.	.193	.041	n.s.
RD		n.s.	.214	.023[a]	n.s.
AD	−.205	.030		n.s.	n.s.
Volume	.236	.016[a]		n.s.	n.s.
Right cingulum proper					
FA		n.s.		n.s.	n.s.
MD	−.372	<.001[a]		n.s.	n.s.
RD	−.276	.005[a]		n.s.	n.s.
AD	−.317	.001[a]		n.s.	n.s.
Volume		n.s.		n.s.	n.s.

Note. n.s. = not significant at .05 α-level.
Abbreviations: AD, axial diffusivity; FA, fractional anisotropy; FDR, false discovery rate; MD, mean diffusivity; RD, radial diffusivity
[a]Significant after FDR correction.

4 | DISCUSSION

The present study examined both the deep bundle portion of the cingulum (referred to here as the cingulum proper) and the U-fibers of the cingulate cortex in children and adolescents with ASDs. This provided greater specificity regarding the structural connectivity in this region than previous ASD studies examining only the cingulum proper and extended the very sparse cingulate U-fiber literature in ASDs. The main findings of this study are as follows: (a) replicated some of the previous findings of altered microstructure in the cingulum proper in ASDs, (b) revealed an altered developmental trajectory in U-fiber macrostructure of the cingulate cortex in ASDs, and (c) found that abnormalities in caudal anterior cingulate U-fiber macrostructure were associated with history of repetitive and restrictive behaviors.

4.1 | Cingulum in ASDs

Several DWI indices suggested compromised white matter microstructure in the left cingulum proper in children and adolescents with ASDs aged 7–18 years, replicating previous studies that also

TABLE 3 Repeated measures ANCOVA results of cingulate U-fiber tracts

	Hemisphere			Age				Group	Hem × age						Hem × group × age					
						Partial corr.					Partial corr.						Partial corr.			
											Left		Right				Left		Right	
Tract/ measure	*p*	eta^2	Direction	*p*	eta^2	*p*	r	*p*	*p*	eta^2	r	*p*	r	*p*	*p*	eta^2	r	*p*	r	*p*
Rostral anterior																				
FA	n.s.			n.s.				n.s.	n.s.						n.s.					
MD	n.s.			n.s.				n.s.	.004[a]	.07	<.01	n.s.	−.21	.026	n.s.					
RD	n.s.			n.s.				n.s.	.008[a]	.06	.01	n.s.	−.20	.032	n.s.					
AD	.007[a]	.06	R > L	n.s.				n.s.	.016	.05	−.01	n.s.	−.20	.038	n.s.					
Volume	.010[a]	.06	L > R	n.s.				n.s.	n.s.						n.s.					
Caudal anterior																				
FA	n.s.			.049	.04	.16	.016	n.s.	n.s.						n.s.					
MD	n.s.			n.s.				n.s.	.039	.04	<.01	n.s.	−.12	n.s.	n.s.					
RD	n.s.			n.s.				n.s.	.049	.04	<.01	n.s.	−.12	n.s.	n.s.					
AD	n.s.			n.s.				n.s.	n.s.						n.s.					
Volume	.002[a]	.09	R > L	n.s.				n.s.	n.s.						n.s.					
Posterior																				
FA	n.s.			n.s.				n.s.	n.s.						n.s.					
MD	n.s.			n.s.				n.s.	n.s.						n.s.					
RD	n.s.			n.s.				n.s.	n.s.						n.s.					
AD	n.s.			n.s.				n.s.	n.s.						n.s.					
Volume	n.s.			.006[a]	.07	−.23	.001	n.s.	n.s.						.011[a]	.06	ASD: −.32	.074	−.32	.013
																	TD: −.33	.017	<.01	n.s.
Isthmus																				
FA	n.s.			n.s.				n.s.	n.s.						n.s.					
MD	n.s.			n.s.				n.s.	n.s.						n.s.					
RD	n.s.			n.s.				n.s.	n.s.						n.s.					
AD	n.s.			n.s.				n.s.	n.s.						n.s.					
Volume	n.s.			n.s.				n.s.	n.s.						.047	.04	ASD: −.21	n.s.	.93	n.s.
																	TD: −.11	n.s.	−.15	n.s.

Note. n.s. = not significant at .05 α-level.

Abbreviations: AD, axial diffusivity; ASD, autism spectrum disorder; FA, fractional anisotropy; FDR, false discovery rate; MD, mean diffusivity; RD, radial diffusivity; TD, typically developing.

[a]Significant after FDR correction.

controlled for head motion (Catani et al., 2016; Fitzgerald et al., 2016; Koolschijn et al., 2016). We found increased RD and MD in the ASD group possibly indicating dysmyelination or demyelination (Alexander, Lee, Lazar, & Field, 2007). Increased RD and MD can also indicate reduced axon packing density (total number within a sampling area), which may be consistent with postmortem studies that found a reduced number of large-caliber axons within the anterior cingulate deep white matter in ASD adults (Zikopoulos et al., 2018; Zikopoulos & Barbas, 2010). There is also some—albeit less consistent—evidence implicating the right cingulum in ASDs (Ameis et al., 2013; Chien, Gau, & Isaac Tseng, 2016; Pugliese et al., 2009; Radua, Via, Catani, & Mataix-Cols, 2011). We did not, however, observe any group-related effects for the right cingulum proper.

We detected some main effects of age (increasing tract volume and decreasing diffusivity) but no group by age interaction. This does not support earlier reports of group by age interactions for cingulum FA (age-related increase in TD but not ASD groups; Ameis et al., 2013; Ikuta et al., 2014). However, small samples in these studies may not have well reflected heterogeneity within the ASD population.

Although our group findings for the cingulum proper were detected only on the left, we found relationships with clinical indices of autism in both hemispheres. In ASDs, reduced right cingulum MD was associated with more severe history of early communication deficits and repetitive and restrictive behaviors, as measured by ADI-R. While the cingulum is commonly thought of as a limbic tract, it has been linked to executive functions including working memory, sustained attention and cognitive control (Bettcher et al., 2016; Chien et al., 2016; Wu et al., 2010). The cingulum has also been linked to executive dysfunction in ASDs, albeit in a small subsample (n = 11, age 18–23 years) where a negative relationship was reported between behavioral regulation and cingulum FA (averaged across hemispheres), which they did not find in the TD group (Ikuta et al., 2014). In our larger and younger sample, we found a significant interaction between groups and GEC score on right cingulum proper MD with the ASD group showing a negative slope compared to the positive slope in the TD group. This could suggest that the neurotypical relationship between cingulum microstructure and executive function may be altered in ASDs, possibly due to compensatory mechanisms or heterogeneity within the disorder. Interestingly, other studies in clinical populations have found associations with executive function in a similar direction, where increased microstructural integrity (FA and generalized FA) of the cingulum was associated with lower working memory function (Chien et al., 2016; Wu et al., 2010). However, the behavioral results for the cingulum proper in this study need to be taken with caution as the associations did not survive correction for multiple statistical tests.

Overall, the present findings suggest a disruption in the deep cingulate white matter in ASDs that may be linked to early symptoms of autism and executive dysfunction. Investigating the cingulum bundle with increased specificity of its anatomy (cingulum sub-bundles) and of the ASD population (i.e., potential sub-types) are needed to help elucidate these findings.

4.2 | Cingulate U-fibers

Little is known about cingulate U-fibers across development. We found hemispheric asymmetry of tract volume for rostral anterior (left-lateralized) and caudal anterior (right-lateralized) cingulate U-fiber divisions. We observed an overall age-related decrease in tract volume for the posterior cingulate U-fibers, in both TD and ASD groups. This pattern of decreasing volume with age contrasts with the age-related volume increase of the cingulum proper (and other long-distance white matter tracts)—both in our study and in longitudinal findings within our age range (Lebel et al., 2012), but is consistent with previous reports on the developmental trajectory of short connections (DiMartino et al., 2014; Hagmann et al., 2010).

4.2.1 | Posterior cingulate U-fibers in ASDs

We detected an altered developmental trajectory in ASDs of tract volume in the posterior cingulate U-fibers (hemisphere × group × age interaction). The right hemisphere tract followed a declining trajectory in volume with age in ASDs whereas the TD group showed a flat trajectory. There was similar decline in both groups in the left hemisphere. This suggests that, in ASDs, right hemisphere U-fiber volume is enlarged in childhood and may end up being reduced relative to typical development in adulthood. Enlarged tract volume may indicate an excess of axons, more branching, and/or less densely packed axons, but the lack of significant microstructural differences in posterior cingulate U-fibers speaks against the latter. Postmortem studies have found abnormalities in white matter underlying cingulate cortex in adults with ASDs, including an increased presence of interstitial neurons underlying posterior cingulate cortex (PCC) in three of eight cases (aged 19, 26, and 54 years) (Oblak, Rosene, Kemper, Bauman, & Blatt, 2011). Another postmortem investigation, examining SWM underlying anterior cingulate cortex (ACC), found greater numbers of small axons in adults with ASDs (30–44 years; eight of nine cases were right hemispheres), attributed to increased axon branching (Zikopoulos & Barbas, 2010). If the PCC were similarly affected (it was not examined in the study) it might help to explain the atypical posterior cingulate U-fiber volume detected in children and adolescents with ASDs in our study.

Extensive U-fiber connections between PCC and adjacent precuneus and paracentral lobules have been shown in tracer studies in monkeys and postmortem dissection in humans (Leichnetz, 2001; Luppino, Matelli, Camarda, & Rizzolatti, 1993; Morecraft & van Hoesen, 1992; Vergani et al., 2014). These short posterior cingulate U-fiber connections may have particular relevance for the default mode network, as the precuneus and PCC are hypothesized to play a central role within this network (Fransson & Marrelec, 2008). Aberrant functional connectivity of the default mode network has been consistently reported in ASDs (Assaf et al., 2010; Lynch et al., 2013), and differences in the U-fibers found here could contribute to this dysfunction. Moreover, the default mode network's structural connectivity appears to be well-developed by early childhood (4–7 years), following a similar trajectory to that seen in primary sensory and

motor networks (Zielinski, Gennatas, Zhou, & Seeley, 2010), whereas its functional connectivity is still developing in children 7–9 years of age (Fair et al., 2008). Thus, alterations of structural connectivity in key areas of the default mode network will likely have important implications for the development of its functional connectivity in ASDs.

4.2.2 | Behavioral correlates

Examination of relationships between cingulate U-fiber tracts and clinical indices revealed that, when controlling for age and data quality (percentage slice dropout), smaller right caudal anterior cingulate U-fiber volume was associated with greater history of repetitive and restrictive behaviors (RRBs) early in life. It is known from axonal tracing studies (Luppino et al., 1993; Morecraft & van Hoesen, 1992) and postmortem dissections (Maldonado et al., 2012; Vergani et al., 2014) that extensive U-fibers connect the cingulate cortex with (pre-) supplementary motor, premotor and primary motor areas and these same cingulate regions also have direct connections to the spinal cord (Dum & Strick, 1991). The U-fiber connections are thus likely to mediate limbic influences on the voluntary motor system (Morecraft & Van Hoesen, 1998). Surprisingly, few studies have investigated cingulate U-fibers and RRBs together. The negative correlation between ADI-R RRB and cingulate U-fiber volume was similarly found for right rostral anterior and left posterior cingulate U-fiber volume, although these correlations did not survive correction for multiple tests. Interestingly, there was no association between ADOS-2 RRB, measuring current symptoms, and U-fiber volume, which suggests that the relationship with volume is linked specifically with history of RRBs in early childhood in ASDs. For microstructure, one small study found that reduced FA, sampled from 2 mm underlying the ACC, in adults with ASDs was linked to higher ratings of RRBs (measured by ADI-R) (Thakkar et al., 2008). We, however, observed a positive correlation of medium effect size between rostral anterior cingulate FA and RRB (measured by ADOS-2), however, it did not survive multiple comparison's correction.

Our results additionally suggest that subdivisions of the cingulate U-fibers may be differentially associated with ASD symptoms, including RRBs (as mentioned above), social deficits, and executive functions, reflecting the diverse functions of the cingulate cortex (Vogt, Finch, & Olson, 1992). Several correlation effects were sub-threshold after FDR correction (and therefore should be viewed with caution). Left caudal anterior and posterior cingulate U-fiber microstructure compromise was related to lower levels of executive functions in TD, suggesting a relationship in the same direction as between the cingulum bundle and executive functions in TD. Larger left posterior cingulate U-fiber volumes and reduced FA, indicating microstructural compromise, were associated with a more severe history of social deficits, as measured by ADI-R. Given that these fibers underlie the PCC, this finding may be related to functional MRI findings linking dysfunction of the PCC with social deficits in ASDs (Di Martino et al., 2009; Salmi et al., 2013). Volume of left rostral and caudal anterior cingulate U-fiber segments were also positively associated with social functioning, measured by the SRS Total, in the TD group.

Interestingly, the findings on the left posterior cingulate U-fiber volume reflect strikingly opposing correlations for ADI-R RRB (negative relationship) and Social (positive relationship) subscales. This may suggest different underlying biological mechanisms, perhaps where a larger volume derives from different anomalies at the microstructural level or from connections with distinct extra-cingulate cortical areas.

Collectively, our results suggest that cingulate U-fibers and cingulum proper are both involved in different ASD symptoms and that the involvement of cingulate white matter is complex. While many of the behavioral findings did not survive statistical correction for multiple tests, the preliminary results are nonetheless intriguing and call for further assessment of cingulate white matter with full consideration of its anatomic specificity. Strengths of the present study include its large ASD sample size and careful matching of diagnostic groups on age, sex, non-verbal IQ and head motion—the latter a significant confound in diffusion MRI studies (Yendiki et al., 2013).

4.3 | Methodological limitations

We detected few cingulum proper streamlines reaching the parahippocampal and entorhinal gyri. The cingulum proper in our study therefore predominantly represented dorsal rather than ventral segments. This may be explained by our seeding strategy from the cingulate cortex (and not parahippocampal and entorhinal gyri), resulting in few surviving streamlines that reached those distant targets. Since we analyzed the cingulum as a single bundle, averaging across cingulum sub-bundles, effects found only within specific sub-bundles may have been masked. Future studies on the cingulum would benefit from sub-dividing the cingulum to further appreciate its complex anatomy (Heilbronner & Haber, 2014; Jones, Christiansen, Chapman, & Aggleton, 2013; Wu, Sun, Wang, Wang, & Ou, 2016).

We used tensor-derived measures (FA, MD, etc.) to quantify white matter microstructure for direct comparisons with existing literature. The limits in the interpretation of the tensor model, primarily due to its inability to resolve fiber crossings, are well-documented (Jones, Knösche & Turner, 2013; Tournier, Mori, & Leemans, 2011). However, tractography itself was performed using the ball-and-stick model rather than the simple tensor model, and allowed for up to three fiber orientations per voxel to account for crossings in fiber orientation.

We included ASD participants with comorbid ADHD, OCD, or anxiety disorders (Table 1), which may affect white matter microstructure in different ways. Psychiatric comorbidities are highly prevalent in children and adolescents with ASDs, estimated at around 70% (Leyfer et al., 2006). Excluding ASD participants with comorbidities would therefore not only reduce the sample size and statistical power, but also result in sample composition that does not well represent the ASD population. As comorbidities vary and occur in different combinations, statistical analyses for effects specific to each comorbidity were unfortunately not possible in the current study.

4.4 | Conclusions

The present study investigated the cingulum proper and cingulate U-fibers in ASDs, providing greater anatomical specificity within the white matter underlying the cingulate cortex. We replicated previous findings of compromised microstructure in the left cingulum in ASDs and found an atypical decline in the right posterior cingulate U-fiber volume driven by enlarged volume in children with ASDs. Smaller right caudal anterior cingulate U-fiber volume was linked to greater early presence of RRBs. Findings suggest that U-fibers of the cingulate cortex, in addition to the cingulum proper, are affected in ASDs and warrant further investigation.

CONFLICT OF INTEREST

The authors report no biomedical financial interests or potential conflicts of interest.

ORCID

Janice Hau https://orcid.org/0000-0002-6919-1971
Inna Fishman https://orcid.org/0000-0002-5873-2365
Ruth A. Carper https://orcid.org/0000-0002-1195-5473
Ralph-Axel Müller https://orcid.org/0000-0001-7299-6757

REFERENCES

Alexander, A. L., Lee, J. E., Lazar, M., & Field, A. S. (2007). Diffusion tensor imaging of the brain. *Neurotherapeutics*, *4*(3), 316–329. http://doi.org/10.1016/j.nurt.2007.05.011

Ameis, S. H., & Catani, M. (2015). Altered white matter connectivity as a neural substrate for social impairment in autism Spectrum disorder. *Cortex*, *62*, 158–181. http://doi.org/10.1016/j.cortex.2014.10.014

Ameis, S. H., Fan, J., Rockel, C., Soorya, L., Wang, A. T., & Anagnostou, E. (2013). Altered cingulum bundle microstructure in autism spectrum disorder. *Acta Neuropsychiatrica*, *25*(5), 275–282. http://doi.org/10.1017/neu.2013.2

American Psychiatric Association (Ed.). (2013). *Diagnostic and statistical manual of mental disorders* (5th ed.). Washington, D.C.: American Psychiatric Publisher.

Amodio, D. M., & Frith, C. D. (2006). Meeting of minds: The medial frontal cortex and social cognition. *Nature Reviews Neuroscience*, *7*(4), 268–277. http://doi.org/10.1038/nrn1884

Andersson, J. L. R., Graham, M. S., Zsoldos, E., & Sotiropoulos, S. N. (2016). Incorporating outlier detection and replacement into a non-parametric framework for movement and distortion correction of diffusion MR images. *NeuroImage*, *141*, 556–572. http://doi.org/10.1016/j.neuroimage.2016.06.058

Andersson, J. L. R., Skare, S., & Ashburner, J. (2003). How to correct susceptibility distortions in spin-echo echo-planar images: Application to diffusion tensor imaging. *NeuroImage*, *20*(2), 870–888. http://doi.org/10.1016/S1053-8119(03)00336-7

Andersson, J. L. R., & Sotiropoulos, S. N. (2016). An integrated approach to correction for off-resonance effects and subject movement in diffusion MR imaging. *NeuroImage*, *125*, 1063–1078. http://doi.org/10.1016/j.neuroimage.2015.10.019

Aoki, Y., Abe, O., Nippashi, Y., & Yamasue, H. (2013). Comparison of white matter integrity between autism spectrum disorder subjects and typically developing individuals: A meta-analysis of diffusion tensor imaging tractography studies. *Molecular Autism*, *4*(1), 25. http://doi.org/10.1186/2040-2392-4-25

Assaf, M., Jagannathan, K., Calhoun, V. D., Miller, L., Stevens, M. C., Sahl, R., … Pearlson, G. D. (2010). Abnormal functional connectivity of default mode sub-networks in autism spectrum disorder patients. *NeuroImage*, *53*(1), 247–256. http://doi.org/10.1016/j.neuroimage.2010.05.067

Behrens, T. E. J., Berg, H. J., Jbabdi, S., Rushworth, M. F. S., & Woolrich, M. W. (2007). Probabilistic diffusion tractography with multiple fibre orientations: What can we gain? *NeuroImage*, *34*(1), 144–155. http://doi.org/10.1016/j.neuroimage.2006.09.018

Behrens, T. E. J., Woolrich, M. W., Jenkinson, M., Johansen-Berg, H., Nunes, R. G., Clare, S., … Smith, S. M. (2003). Characterization and propagation of uncertainty in diffusion-weighted MR imaging. *Magnetic Resonance in Medicine*, *50*(5), 1077–1088. http://doi.org/10.1002/mrm.10609

Belmonte, M. K., Allen, G., Beckel-Mitchener, A., Boulanger, L. M., Carper, R. a., & Webb, S. J. (2004). Autism and abnormal development of brain connectivity. *The Journal of Neuroscience*, *24*(42), 9228–9231. http://doi.org/10.1523/JNEUROSCI.3340-04.2004

Benjamini, Y., & Hochberg, Y. (1995). Controlling the false discovery rate: A practical and powerful approach to multiple testing. *Journal of the Royal Statistical Society B*, *57*(1), 289–300. http://doi.org/10.2307/2346101

Bettcher, B. M., Mungas, D., Patel, N., Elofson, J., Dutt, S., Wynn, M., … Kramer, J. H. (2016). Neuroanatomical substrates of executive functions: Beyond prefrontal structures. *Neuropsychologia*, *85*, 100–109. http://doi.org/10.1016/j.neuropsychologia.2016.03.001

Billeci, L., Calderoni, S., Tosetti, M., Catani, M., & Muratori, F. (2012). White matter connectivity in children with autism spectrum disorders: A tract-based spatial statistics study. *BMC Neurology*, *12*, 148. http://doi.org/10.1186/1471-2377-12-148

Bush, G., Luu, P., & Posner, M. I. (2000). Cognitive and emotional influences in anterior cingulate cortex. *Trends in Cognitive Sciences*, *4*(6), 215–222. http://doi.org/10.1016/S1364-6613(00)01483-2

Catani, M., Dell'Acqua, F., Budisavljevic, S., Howells, H., Thiebaut de Schotten, M., Froudist-Walsh, S., … Murphy, D. G. M. (2016). Frontal networks in adults with autism spectrum disorder. *Brain*, *139*(2), 616–630. http://doi.org/10.1093/brain/awv351

Chiang, H. L., Chen, Y. J., Lin, H. Y., Tseng, W. Y. I., & Gau, S. S. F. (2017). Disorder-specific alteration in white matter structural property in adults with autism spectrum disorder relative to adults with ADHD and adult controls. *Human Brain Mapping*, *38*(1), 384–395. http://doi.org/10.1002/hbm.23367

Chien, H.-Y., Gau, S. S.-F., & Isaac Tseng, W.-Y. (2016). Deficient visuospatial working memory functions and neural correlates of the default-mode network in adolescents with autism spectrum disorder. *Autism Research*, *9*(10), 1058–1072. http://doi.org/10.1002/aur.1607

Constantino, J. (2002). *The social responsiveness scale*. Los Angeles: Western Psychological Services.

d'Albis, M.-A., Guevara, P., Guevara, M., Laidi, C., Boisgontier, J., Sarrazin, S., … Houenou, J. (2018). Local structural connectivity is associated with social cognition in autism spectrum disorder. *Brain*, *141*, 3472–3481. http://doi.org/10.1093/brain/awy275

Desikan, R. S., Ségonne, F., Fischl, B., Quinn, B. T., Dickerson, B. C., Blacker, D., … Killiany, R. J. (2006). An automated labeling system for subdividing the human cerebral cortex on MRI scans into gyral based regions of interest. *NeuroImage*, *31*(3), 968–980. http://doi.org/10.1016/j.neuroimage.2006.01.021

Di Martino, A., Ross, K., Uddin, L. Q., Sklar, A. B., Castellanos, F. X., & Milham, M. P. (2009). Functional brain correlates of social and nonsocial processes in autism spectrum disorders: An activation likelihood estimation meta-analysis. *Biological Psychiatry*, *65*(1), 63–74. http://doi.org/10.1016/j.biopsych.2008.09.022

DiMartino, A., Fair, D. A., Kelly, C., Satterthwaite, T. D., Castellanos, F. X., Thomason, M. E., … Milham, M. P. (2014). Unraveling the miswired connectome: A developmental perspective. *Neuron*, *83*(6), 1335–1353. http://doi.org/10.1016/j.neuron.2014.08.050

Dum, R. P., & Strick, P. L. (1991). The origin of corticospinal projections from the premotor areas in the frontal lobe. *Journal of Neuroscience*, *11*(3), 667–689. http://doi.org/S0022510X0200268X

Ellmore, T. M., Li, H., Xue, Z., Wong, S. T. C., & Frye, R. E. (2013). Tract-based spatial statistics reveal altered relationship between non-verbal reasoning abilities and white matter integrity in autism spectrum disorder. *Journal of the International Neuropsychological Society*, *19*(6), 723–728. http://doi.org/10.1017/S1355617713000325

Fair, D. A., Cohen, A. L., Dosenbach, N. U. F., Church, J. A., Miezin, F. M., Barch, D. M., … Schlaggar, B. L. (2008). The maturing architecture of the brain's default network. *Proceedings of the National Academy of Sciences of the United States of America*, *105*(10), 4028–4032. http://doi.org/10.1073/pnas.0800376105

Fitzgerald, J., Gallagher, L., & McGrath, J. (2016). Widespread disrupted white matter microstructure in autism spectrum disorders. *Journal of Autism and Developmental Disorders*. http://doi.org/10.1007/s10803-016-2803-8. [Epub ahead of print]

Fransson, P., & Marrelec, G. (2008). The precuneus/posterior cingulate cortex plays a pivotal role in the default mode network: Evidence from a partial correlation network analysis. *NeuroImage*, *42*(3), 1178–1184. http://doi.org/10.1016/j.neuroimage.2008.05.059

Gioia, G., Isquith, P., Guy, S., & Kenworthy, L. (2016). *Behavior rating inventory of executive function, (BRIEF-2)*. Retrieved from http://www4.parinc.com/WebUploads/samplerpts/BRIEF2FactSheet.pdf

Greve, D. N., & Fischl, B. (2009). Accurate and robust brain image alignment using boundary-based registration. *NeuroImage*, *48*(1), 63–72. http://doi.org/10.1016/j.neuroimage.2009.06.060

Hagmann, P., Sporns, O., Madan, N., Cammoun, L., Pienaar, R., Wedeen, V. J., … Grant, P. E. (2010). White matter maturation reshapes structural connectivity in the late developing human brain. *Proceedings of the National Academy of Sciences of the United States of America*, *107*(44), 19067–19072. http://doi.org/10.1073/pnas.1009073107

Heilbronner, S. R., & Haber, S. N. (2014). Frontal cortical and subcortical projections provide a basis for segmenting the cingulum bundle: Implications for neuroimaging and psychiatric disorders. *Journal of Neuroscience*, *34*(30), 10041–10054. http://doi.org/10.1523/JNEUROSCI.5459-13.2014

Herbert, M. R., Ziegler, D. A., Makris, N., Filipek, P. A., Kemper, T. L., Normandin, J. J., … Caviness, V. S., Jr. (2004). Localization of white matter volume increase in autism and developmental language disorder. *Annals of Neurology*, *55*, 530–540. http://doi.org/10.1002/ana.20032

Ikuta, T., Shafritz, K. M., Bregman, J., Peters, B., Gruner, P., Malhotra, A. K., & Szeszko, P. R. (2014). Abnormal cingulum bundle development in autism: A probabilistic Tractography study. *Psychiatry Research*, *30*(221(1)), 63–68. http://doi.org/10.1016/j.jacc.2007.01.076.White

Jones, D. K., Christiansen, K. F., Chapman, R. J., & Aggleton, J. P. (2013). Distinct subdivisions of the cingulum bundle revealed by diffusion MRI fibre tracking: Implications for neuropsychological investigations. *Neuropsychologia*, *51*(1), 67–78. http://doi.org/10.1016/j.neuropsychologia.2012.11.018

Jones, D. K., Knösche, T. R., & Turner, R. (2013). White matter integrity, fiber count, and other fallacies: The do's and don'ts of diffusion MRI. *NeuroImage*, *73*, 239–254. http://doi.org/10.1016/j.neuroimage.2012.06.081

Keedwell, P. A., Doidge, A. N., Meyer, M., Lawrence, N., Lawrence, A. D., & Jones, D. K. (2016). Subgenual cingulum microstructure supports control of emotional Conflict. *Cerebral Cortex*, *26*(6), 2850–2862. http://doi.org/10.1093/cercor/bhw030

Koldewyn, K., Yendiki, A., Weigelt, S., Gweon, H., Julian, J., Richardson, H., … Kanwisher, N. (2014). Differences in the right inferior longitudinal fasciculus but no general disruption of white matter tracts in children with autism spectrum disorder. *Proceedings of the National Academy of Sciences of the United States of America*, *111*(5), 1981–1986. http://doi.org/10.1073/pnas.1324037111

Koolschijn, P. C. M. P., Caan, M. W. A., Teeuw, J., Olabarriaga, S. D., & Geurts, H. M. (2016). Age-related differences in autism: The case of white matter microstructure. *Human Brain Mapping*, *00*(April), 1–15. http://doi.org/10.1002/hbm.23345

Le Couteur, A., Lord, C., & Rutter, M. (2003). *The autism diagnostic interview-revised (ADI-R)*. Los Angeles, CA: Western Psychological Services.

Lebel, C., Gee, M., Camicioli, R., Wieler, M., Martin, W., & Beaulieu, C. (2012). Diffusion tensor imaging of white matter tract evolution over the lifespan. *NeuroImage*, *60*(1), 340–352. http://doi.org/10.1016/j.neuroimage.2011.11.094

Leichnetz, G. R. (2001). Connections of the medial posterior parietal cortex (area 7m) in the monkey. *Anatomical Record*, *263*(2), 215–236. http://doi.org/10.1002/ar.1082

Leyfer, O. T., Folstein, S. E., Bacalman, S., Davis, N. O., Dinh, E., Morgan, J., … Lainhart, J. E. (2006). Comorbid psychiatric disorders in children with autism: Interview development and rates of disorders. *Journal of Autism and Developmental Disorders*, *36*(7), 849–861. http://doi.org/10.1007/s10803-006-0123-0

Lord, C., Rutter, M., DiLavore, P., & Risi, S. (2002). *The autism diagnostic observation scale (ADOS)*. Los Angeles, CA: Western Psychological.

Luppino, G., Matelli, M., Camarda, R., & Rizzolatti, G. (1993). Corticocortical connections of area F3 (SMA-proper) and area F6 (pre-SMA) in the macaque monkey. *Journal of Comparative Neurology*, *338*(1), 114–140. http://doi.org/10.1002/cne.903380109

Lynch, C. J., Uddin, L. Q., Supekar, K., Khouzam, A., Phillips, J., & Menon, V. (2013). Default mode network in childhood autism: Posteromedial cortex heterogeneity and relationship with social deficits. *Biological Psychiatry*, *74*(3), 212–219. http://doi.org/10.1016/j.biopsych.2012.12.013

Maldonado, I. L., Mandonnet, E., & Duffau, H. (2012). Dorsal fronto-parietal connections of the human brain: A fiber dissection study of their composition and anatomical relationships. *Anatomical Record*, *295*(2), 187–195. http://doi.org/10.1002/ar.21533

Metzler-Baddeley, C., Jones, D. K., Steventon, J., Westacott, L., Aggleton, J. P., & O'Sullivan, M. J. (2012). Cingulum microstructure predicts cognitive control in older age and mild cognitive impairment. *Journal of Neuroscience*, *32*(49), 17612–17619. http://doi.org/10.1523/JNEUROSCI.3299-12.2012

Morecraft, R. J., & van Hoesen, G. W. (1992). Cingulate input to the primary and supplementary motor cortices in the rhesus monkey: Evidence for somatotopy in areas 24c and 23c. *Journal of Comparative Neurology*, *322*(4), 471–489. http://doi.org/10.1002/cne.903220403

Morecraft, R. J., & Van Hoesen, G. W. (1998). Convergence of limbic input to the cingulate motor cortex in the rhesus monkey. *Brain Research Bulletin*, *45*(2), 209–232. http://doi.org/10.1016/S0361-9230(97)00344-4

Oblak, A. L., Rosene, D. L., Kemper, T. L., Bauman, M. L., & Blatt, G. J. (2011). Altered posterior cingulate cortical cyctoarchitecture, but normal density of neurons and interneurons in the posterior cingulate cortex and fusiform gyrus in autism. *Autism Research*, *4*(3), 200–211. http://doi.org/10.1002/aur.188

Oldfield, R. C. (1971). The assessment and analysis of handedness: The Edinburgh inventory. *Neuropsychologia*, *9*(1), 97–113. http://doi.org/10.1016/0028-3932(71)90067-4

Paus, T. (2001). Primate anterior cingulate cortex: Where motor control, drive and cognition interface. *Nature Reviews Neuroscience*, *2*(June), 417–424. http://doi.org/10.1038/35077500

Pugliese, L., Catani, M., Ameis, S., Dell'Acqua, F., de Schotten, M. T., Murphy, C., … Murphy, D. G. M. (2009). The anatomy of extended limbic pathways in Asperger syndrome: A preliminary diffusion tensor imaging tractography study. *NeuroImage*, *47*(2), 427–434. http://doi.org/10.1016/j.neuroimage.2009.05.014

Radua, J., Via, E., Catani, M., & Mataix-Cols, D. (2011). Voxel-based meta-analysis of regional white-matter volume differences in autism spectrum disorder versus healthy controls. *Psychological Medicine*, *41*(7), 1539–1550. http://doi.org/10.1017/S0033291710002187

Salmi, J., Roine, U., Glerean, E., Lahnakoski, J., Nieminen-von Wendt, T., Tani, P., … Rintahaka, P. (2013). The brains of high functioning autistic individuals do not synchronize with those of others. *NeuroImage: Clinical*, *3*, 489–497.

Schmahmann, J. D., & Pandya, D. N. (2006). *Fiber pathways of the brain*. New York: Oxford University Press.

Shukla, D. K., Keehn, B., Smylie, D. M., & Müller, R.-A. (2011). Microstructural abnormalities of short-distance white matter fiber tracts in autism spectrum disorder. *Neuropsychologia*, *49*(5), 1378–1382. http://doi.org/10.1016/j.pestbp.2011.02.012.Investigations

Simonoff, E., Pickles, A., Charman, T., Chandler, S., Loucas, T., & Baird, G. (2008). Psychiatric disorders in children with autism spectrum disorders: Prevalence, comorbidity, and associated factors in a population-derived sample. *Journal of the American Academy of Child and Adolescent Psychiatry*, *47*(8), 921–929. http://doi.org/10.1097/CHI.0b013e318179964f

Solders, S. K., Carper, R. A., & Müller, R. A. (2017). White matter compromise in autism? Differentiating motion confounds from true differences in diffusion tensor imaging. *Autism Research*, *10*, 1–15. http://doi.org/10.1002/aur.1807

Sundaram, S. K., Kumar, A., Makki, M. I., Behen, M. E., Chugani, H. T., & Chugani, D. C. (2008). Diffusion tensor imaging of frontal lobe in autism spectrum disorder. *Cerebral Cortex*, *18*(11), 2659–2665. http://doi.org/10.1093/cercor/bhn031

Thakkar, K. N., Polli, F. E., Joseph, R. M., Tuch, D. S., Hadjikhani, N., Barton, J. J. S., & Manoach, D. S. (2008). Response monitoring, repetitive behaviour and anterior cingulate abnormalities in autism spectrum disorders (ASD). *Brain*, *131*(9), 2464–2478. http://doi.org/10.1093/brain/awn099

Thompson, A., Murphy, D., Dell'Acqua, F., Ecker, C., McAlonan, G., Howells, H., … Lombardo, M. V. (2017). Impaired communication between the motor and somatosensory homunculus is associated with poor manual dexterity in autism Spectrum disorder. *Biological Psychiatry*, *81*(3), 211–219. http://doi.org/10.1016/j.biopsych.2016.06.020

Tournier, J. J.-D., Mori, S., & Leemans, A. (2011). Diffusion tensor imaging and beyond. *Magnetic Resonance in Medicine*, *65*(6), 1532–1556. http://doi.org/10.1002/mrm.22924

Travers, B. G., Adluru, N., Ennis, C., Tromp, D. P. M., Destiche, D., Doran, S., … Alexander, A. L. (2012). Diffusion tensor imaging in autism spectrum disorder: A review. *Autism Research*, *5*(5), 289–313. http://doi.org/10.1002/aur.1243

Vergani, F., Lacerda, L., Martino, J., Attems, J., Morris, C., Mitchell, P., … Dell'Acqua, F. (2014). White matter connections of the supplementary motor area in humans. *Journal of Neurology, Neurosurgery and Psychiatry*, *85*(12), 1377–1385. http://doi.org/10.1136/jnnp-2013-307492

Vogt, B. A., Finch, D. M., & Olson, C. R. (1992). Functional heterogeneity in cingulate cortex: The anterior executive and posterior evaluative regions. *Cerebral Cortex*, *2*(March), 435–443.

Wechsler, D. (1999). *Manual for the Wechsler abbreviated intelligence scale (WASI)*. San Antonio, TX: The Psychological Corporation.

Weinstein, M., Ben-Sira, L., Levy, Y., Zachor, D. A., Itzhak, E. B., Artzi, M., … Bashat, D. B. (2011). Abnormal white matter integrity in young children with autism. *Human Brain Mapping*, *32*(4), 534–543. http://doi.org/10.1002/hbm.21042

Wu, T. C., Wilde, E. A., Bigler, E. D., Yallampalli, R., McCauley, S. R., Troyanskaya, M., … Levin, H. S. (2010). Evaluating the relationship between memory functioning and cingulum bundles in acute mild traumatic brain injury using diffusion tensor imaging. *Journal of Neurotrauma*, *27*(2), 303–307. http://doi.org/10.1089/neu.2009.1110

Wu, Y., Sun, D., Wang, Y., Wang, Y., & Ou, S. (2016). Segmentation of the cingulum bundle in the human brain: A new perspective based on DSI Tractography and Fiber dissection study. *Frontiers in Neuroanatomy*, *10*(September), 1–16. http://doi.org/10.3389/fnana.2016.00084

Xiao, Z., Qiu, T., Ke, X., Xiao, X., Xiao, T., Liang, F., … Liu, Y. (2014). Autism spectrum disorder as early neurodevelopmental disorder: Evidence from the brain imaging abnormalities in 2-3 years old toddlers. *Journal of Autism and Developmental Disorders*, *44*(7), 1633–1640. http://doi.org/10.1007/s10803-014-2033-x

Yakovlev, P. I., & Locke, S. (1961). Limbic nuclei of thalamus and connections of limbic cortex: III. Corticocortical connections of the anterior cingulate gyrus, the cingulum, and the subcallosal bundle in monkey. *Archives of neurology*, *5*(4), 364–400.

Yendiki, A., Koldewyn, K., Kakunoori, S., Kanwisher, N., & Fischl, B. (2013). Spurious group differences due to head motion in a diffusion MRI study. *NeuroImage*, *88c*, 79–90. http://doi.org/10.1016/j.neuroimage.2013.11.027

Zielinski, B. A., Gennatas, E. D., Zhou, J., & Seeley, W. W. (2010). Network-level structural covariance in the developing brain. *Proceedings of the National Academy of Sciences*, *107*(42), 18191–18196. http://doi.org/10.1073/pnas.1003109107

Zikopoulos, B., & Barbas, H. (2010). Changes in prefrontal axons may disrupt the network in autism. *Journal of Neuroscience*, *30*(44), 14595–14609. http://doi.org/10.1523/JNEUROSCI.2257-10.2010

Zikopoulos, B., Garcia-Cabezas, M. A., & Barbas, H. (2018). Parallel trends in cortical gray and white matter architecture and connections in primates allow fine study of pathways in humans and reveal network disruptions in autism. *PLoS Biology*, *16*, e2004559. http://doi.org/10.1371/journal.pbio.2004559

SUPPORTING INFORMATION

Additional supporting information may be found online in the Supporting Information section at the end of this article.

How to cite this article: Hau J, Aljawad S, Baggett N, Fishman I, Carper RA, Müller R-A. The cingulum and cingulate U-fibers in children and adolescents with autism spectrum disorders. *Hum Brain Mapp*. 2019;40:3153–3164. https://doi.org/10.1002/hbm.24586